Mössbauer Study of Cobalt-Zinc Ferrites

G. A. Petitt
Department of Physics, Georgia State University, Atlanta, Georgia 30303

and

D. W. Forester
Naval Research Laboratory, Washington, D.C. 20390

(Received 15 October 1970)

Samples of the cobalt-zinc ferrite series $Co_{1-x}Zn_xFe_2O_4$ have been studied by the Mössbauer-effect technique at 4 °K, in magnetic fields from 0 to 80 kOe, covering the full range of zinc content. The cation distributions and the hyperfine fields at ^{57}Fe nuclei in A and B sites have been determined as a function of Zn concentration. Canted spin structures associated with Fe^{3+} ions are observed for all samples at 4 °K. At large values of x the resolved spectral features provide distinct evidence of localized spin canting with a distribution of canting angles determined by the statistical distribution of nonmagnetic (Zn^{2+}) neighboring ions. For low concentrations of nonmagnetic ions, the distribution of hyperfine fields is, to a good approximation, independent of the distribution of canting angles, and these spectra are analyzed in terms of supertransferred hyperfine fields from neighboring ions. The temperature dependence of the hyperfine magnetic field has been determined for several samples. For samples with $x = 0.4$ and $x = 0.6$, the Néel temperatures are found to be (513 ± 5) and (322 ± 5) °K, respectively.

I. INTRODUCTION

Solid solutions of the spinel $Co_{1-x}Zn_xFe_2O_4$ may be prepared with values of x between 0 and 1. The Fe^{3+}, Co^{2+}, and Zn^{2+} cations are distributed among octahedral (B) and tetrahedral (A) interstitial sites of the face-centered-cubic oxygen lattice. $ZnFe_2O_4$ ($x = 1$) is generally assumed to be a "normal" spinel with all Fe^{3+} ions on B sites and all Zn^{2+} ions on A sites.[1] In $CoFe_2O_4$ ($x = 0$), the site preferences lead to a predominantly "inverse" structure with Co^{2+} ions mainly on B sites and Fe^{3+} ions distributed almost equally between A and B sites. The inversion is not complete in $CoFe_2O_4$ and the degree of inversion depends on previous heat treatment.[2] As zinc replaces cobalt between $x = 0$ and $x = 1$, Zn^{2+} ions appear to preferentially enter tetrahedral positions, while the Fe^{3+} ions displaced from these tetrahedral sites enter the octahedral sublattice. However, the exact cation distributions have not been determined experimentally.

$CoFe_2O_4$ is ferrimagnetic below its Néel temperature (~ 860 °K),[1] while $ZnFe_2O_4$ is antiferromagnetic below about 9 °K.[1,3] The magnetic order of $ZnFe_2O_4$ is a result of antiferromagnetic intersublattice exchange J_{BB}, whereas the ferrimagnetism of $CoFe_2O_4$ is due to antiferromagnetic intrasublattice exchange J_{AB} which is larger than J_{BB}. In the latter case the magnetic moments of ions on the B sublattice are aligned parallel to the direction of the net magnetization and antiparallel to the moments on the A sublattice. The variation of the low-temperature saturation magnetization in zinc-substituted cobalt ferrite has been determined by several workers.[4,5] The readjustment of cations in the lattice produces an initial constant increase of magnetization with increasing zinc content. Near $x = 0.5$, however, the magnetization levels off and then decreases to zero for $x = 1$. The reason for this decrease has been explained in terms of various models including (a) occupation of the B sites by Zn^{2+} ions,[4-6] (b) development of paramagnetic clusters,[7,8] and (c) the occurrence of noncollinear spin structures.[9-16] A preliminary report by the authors[17] has indicated that noncollinear magnetic structure is an important part of the explanation of this behavior in $Co_{1-x}Zn_xFe_2O_4$. Recent neutron-diffraction[18] and Mössbauer-effect (ME)[19] studies have shown that canting is also present in the similar $Ni_{1-x}Zn_xFe_2O_4$ system. The canting in that system is interpreted in terms of a uniform Yaffet-Kittel[9] triangular-type magnetic ordering of spins on the B sublattice. On the other hand, recent theoretical treatments of canting in spinels and garnets, which include the effects of chemical disorder, predict a localized spin "flipping"[11,12] or canting.[13-16] Whether or not an ion is flipped or the extent to which it is canted out of alignment with the sublattice magnetization depends on the number of nonmagnetic ions that are nearest neighbors to it.

Other investigations have recently been made of ferrimagnetic and antiferromagnetic spinels using ME and NMR techniques.[2,20-24] These investigations have shown that, in general, different hyperfine fields and isomer shifts exist at the nuclei of Fe^{3+} ions at A and B sites. In several cases evidence has been found for contributions to the hyperfine magnetic fields at nuclei in these sites due to supertransferred electron spin density.[2,21]

The purpose of this paper is to present the re-

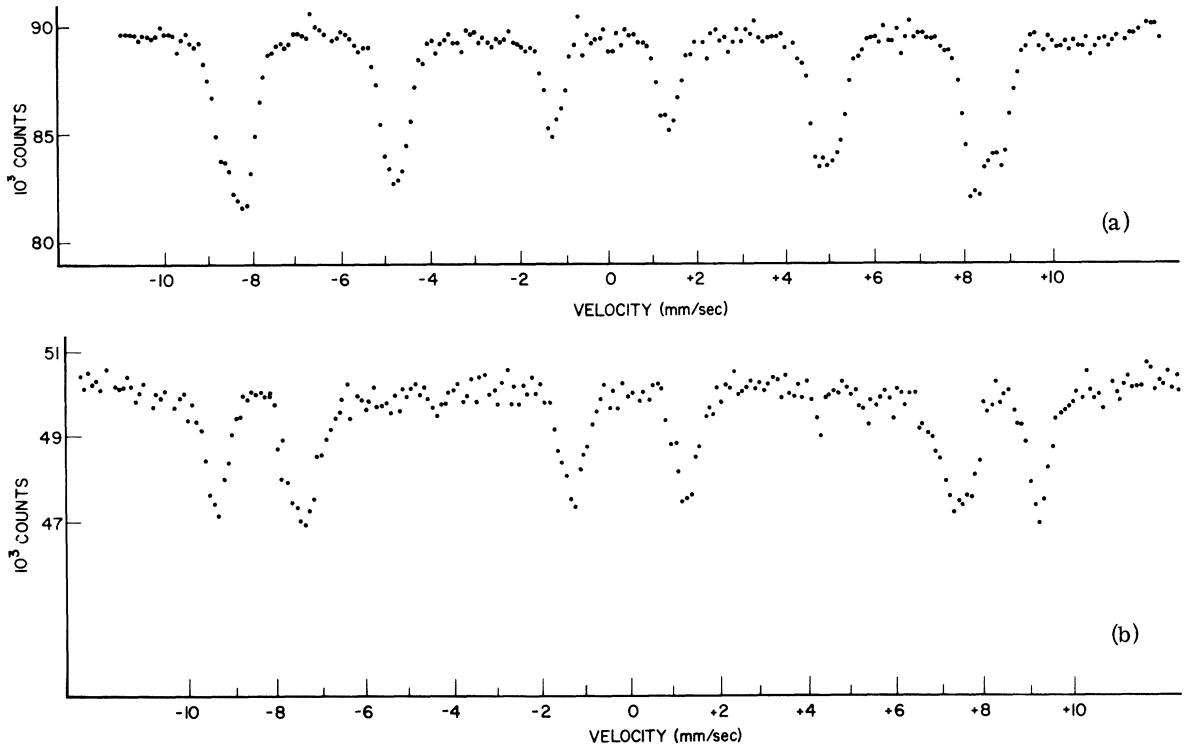

FIG. 1. Mössbauer spectra of $CoFe_2O_4$ with (a) zero external magnetic field and (b) an external magnetic field $H_0 = 80$ kOe applied parallel to the direction of γ-ray emission.

sults of a systematic ME study on ^{57}Fe in $Co_{1-x}Zn_xFe_2O_4$ as a function of Zn^{2+} concentration to determine cation distributions, possible canted spin structures, and information about supertransferred hyperfine (STH) interactions at both A and B sites.

In Sec. II we describe the experimental setup and preparation of the investigated materials. The cation distributions are discussed in Sec. III. A discussion of the canted spin structures found for these samples is given in Sec. IV, and in Sec. V the hyperfine fields are discussed. The temperature dependence of the spectra is discussed in Sec. VI.

II. EXPERIMENTAL

The materials were prepared by the following technique: Appropriate amounts of the nitrates of Fe, Co, and Zn were dissolved in water. The carbonates of Fe, Co, and Zn were then precipitated out of solution by adding ammonium carbonate. This technique assured a very homogeneous mixture of the materials. After thorough rinsing, the material was prefired at 900 °C in air to drive off the carbon as carbon monoxide. The resulting porous materials were pressed into pellets and refired in air for 2 h at 1250 °C. The samples were then coiled at the rate of 1 °C/min. The short firing time was used because of the volatility of CoO at high temperatures. Powder x-ray–diffraction patterns indicated that all samples had the spinel structure with no evidence of impurities or separate phases.

Mössbauer spectra were taken using a constant acceleration drive, driven in synchronization with a 512-channel analyzer. The source was ^{57}Co plated on platinum. Calibration spectra were taken with an enriched ^{57}Fe foil using a value of 330 kOe for the effective nuclear hyperfine field H_{eff} at room temperature. The source temperature was maintained at 200 °K. In order to investigate the hyperfine spectra under conditions of saturation, the sample temperature was maintained between 2 and 4 °K. Large magnetic fields were produced both by a superconducting solenoid and a Bitter-type solenoid.[25] Measurements as a function of temperature were made using a liquid-helium cryostat with variable-temperature tail and a variable-temperature oven.

III. CATION DISTRIBUTIONS

Representative ME spectra from this study with external magnetic fields applied parallel to the direction of γ-ray emission are shown in Figs. 1–4. The spectra show completely resolved splittings of the outer lines of the spectrum as the applied field adds to the magnetic hyperfine fields at A sites and subtracts from the hyperfine fields at B sites. The relative numbers of Fe ions in A and B sites are

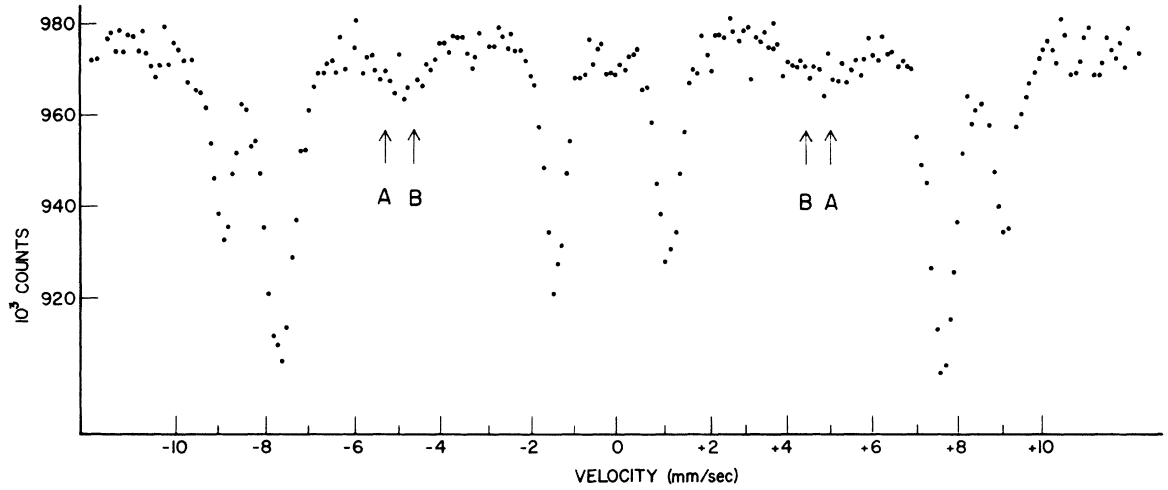

FIG. 2. Mössbauer spectrum of $Co_{0.6}Zn_{0.4}Fe_2O_4$ in an external magnetic field $H_0 = 50$ kOe. The arrows labelled A and B indicate the positions of the $\Delta m = 0$ lines for A- and B-site ^{57}Fe nuclei, respectively.

determined from the ratios of the areas of these outer peaks. From this the number of Co and Zn ions on A and B sites may be inferred.

The simplest case to consider is $CoFe_2O_4$ which involves only one other cation in addition to Fe^{3+} ions. The ME spectra of $CoFe_2O_4$ both with and without an external field are shown in Fig. 1. As observed previously,[2] the ratio of the area of the outer A- and B-sublattice peaks indicates an excess of Fe^{3+} ions on B sites and hence a fraction y of Co^{2+} ions on A sites. This distribution may be described by the chemical formula

$$(Fe_{1-y}Co_y)\,[Co_{1-y}Fe_{1+y}]O_4\,, \qquad (1)$$

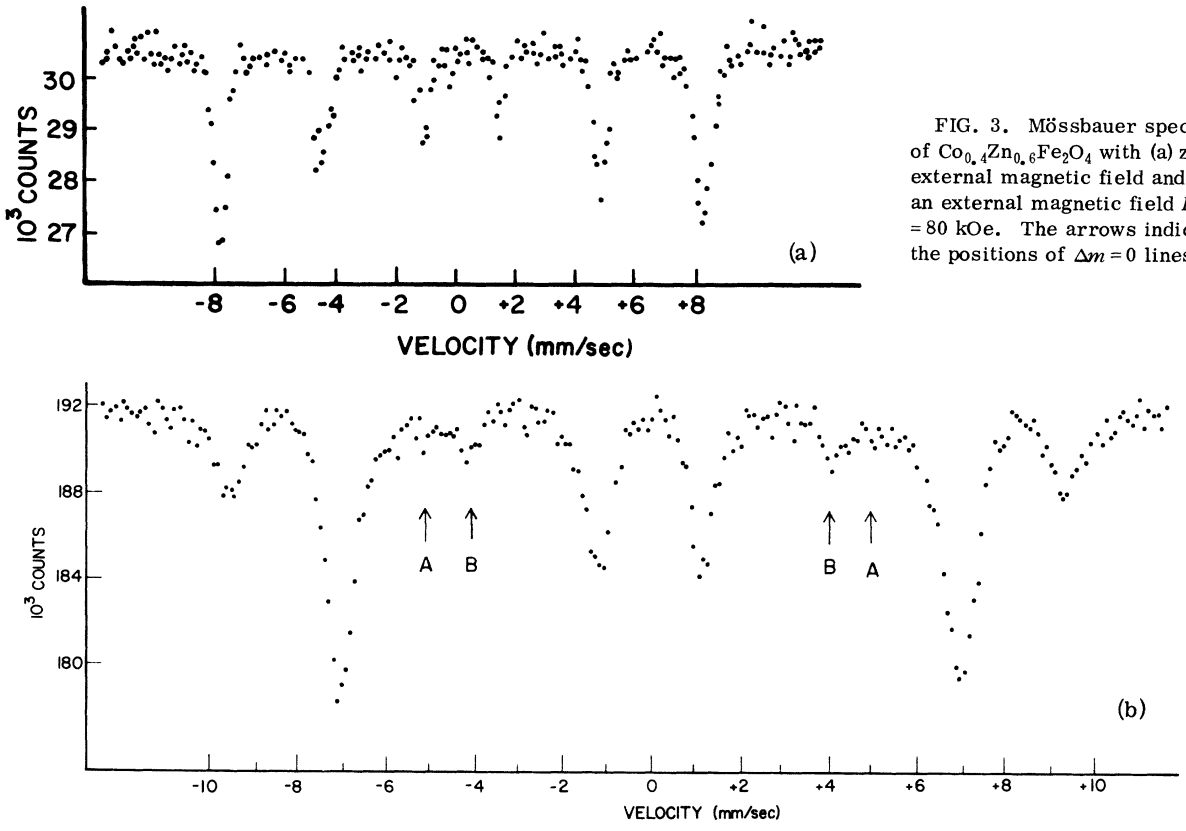

FIG. 3. Mössbauer spectra of $Co_{0.4}Zn_{0.6}Fe_2O_4$ with (a) zero external magnetic field and (b) an external magnetic field $H_0 = 80$ kOe. The arrows indicate the positions of $\Delta m = 0$ lines.

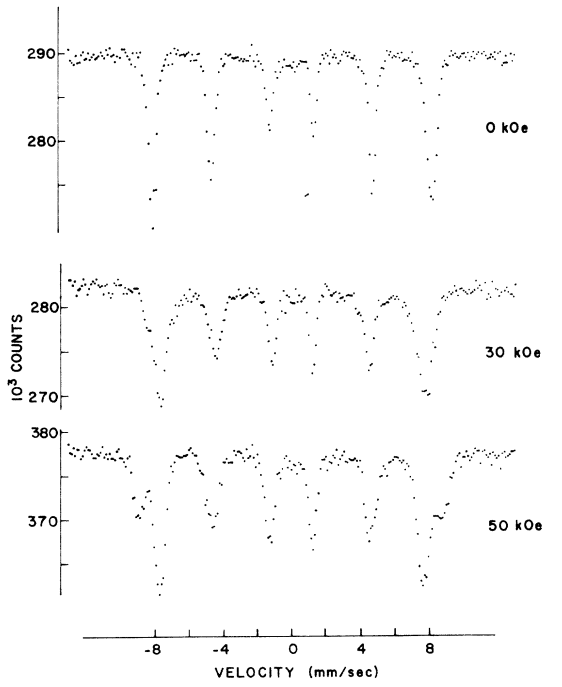

FIG. 4. Mössbauer spectra of $Co_{0.2}Zn_{0.8}Fe_2O_4$ with (a) zero external magnetic field, (b) an external magnetic field $H_0 = 30$ kOe, and (c) an external field $H_0 = 50$ kOe.

where () denotes A sites and [] denotes B sites. The value of y calculated from our data using this formula is $y = 0.19$ which is comparable to the value of 0.24 obtained by Sawatzky *et al.*[2] for a sample quenched rapidly after firing. Although our sample was cooled slowly after firing, the short firing time (2 h) was apparently not sufficient to bring about a very high degree of inversion. Nevertheless, this lack of inversion in $CoFe_2O_4$ leads to a distribution of hyperfine fields which is beneficial for studying the effects of STH interactions as discussed later.

When zinc is added to the system, the outermost A-site peaks, shown in Figs. 1–4, decrease in intensity with respect to the B-site peaks. This trend is consistent with the picture that Zn^{2+} ions enter tetrahedral sites and Fe^{3+} ions at tetrahedral sites are displaced to octahedral sites. For a completely inverse structure the chemical formula for the zinc-substituted ferrite system would be identical with Eq. (1) except with y, the fraction of Co^{2+} ions at A sites, replaced by x, the zinc concentration. If the system is not completely inverse the formula is instead a combination of the two:

$$(Zn_xFe_{1-x-y}Co_y)\,[Co_{1-x-y}Fe_{1+x+y}]O_4\,. \qquad (2)$$

For $0 \le x \le 0.6$ the values of y for a given x were calculated from the area ratios of the outer peaks shown in Figs. 1–4 and using Eq. (2). From the values of y, shown in Table I, it is seen that the tendency for Co^{2+} ions to be in A sites, as observed at $x = 0$, quickly disappears as zinc is added. For $x = 0.8$, the A-site peak intensity is relatively too large to be explained in terms of Eq. (2). This discrepancy could be explained if part of the Zn^{2+} ions at the larger zinc concentrations enter B instead of A sites. However, a careful analysis of unresolved structure in this spectrum, discussed later in Sec. IV, indicates that the discrepancy is primarily due to large-angle localized canting of spins on the B sublattice. A value of $y = 0$ was therefore assumed for calculations at this concentration. With this assumption, the data in Table I indicate that except near $x = 0$, the general behavior as a function of added zinc is that of an inverse ferrite with substitution in the tetrahedral sites.

IV. SPIN CONFIGURATIONS

The saturation magnetic moment per molecular unit of $Co_{1-x}Zn_xFe_2O_4$ as a function of x at 0 °K is given in Fig. 6. The straight-line extrapolation of the experimental curve indicates the expected curve for a Néel collinear arrangement of spins with the spins of ions in B sites parallel to each other and antiparallel to the spins of ions in A sites. The experimental curve begins to deviate from the straight line at $x = 0.4$ and then decreases rapidly with increasing x beyond $x = 0.6$.

Several possible explanations for this reduction have been proposed, including superparamagnetic behavior,[7,8] the presence of zinc ions in both A and B sites,[4–6] or the canting of the sublattice magnetic moments.[11–16] However, as discussed in Sec. III, zinc ions appear to enter only the A sites and, as discussed below in Sec. VI, there is no strong evidence for superparamagnetic cluster effects in Co-Zn ferrites at low temperatures. Instead, the data presented in this paper show that the primary cause of this reduction is canting of the sublattice moments.

The presence of $\Delta m = 0$ lines in ME spectra taken in an external magnetic field parallel to the direction of γ-ray transmission provides unambiguous evidence for the existence of canting angles between individual moments and the direction of the net sublattice magnetization. As shown in Figs. 1–4, all the samples in this study have at least trace amounts of $\Delta m = 0$ lines present. These lines increase in intensity from being barely discernable in $CoFe_2O_4$ [Fig. 1(b)] to being comparable with the outermost peaks in $Co_{0.2}Zn_{0.8}Fe_2O_4$ in Figs. 4 and

TABLE I. Cation distributions in $Co_{1-x}Zn_xFe_2O_4$ giving fraction y of Co ions at A sites.

x	0.0	0.2	0.4	0.6	0.8
y	0.19 ± 0.02	0.10 ± 0.02	0.0 ± 0.04	0.0 ± 0.04	0.0 ± 0.04

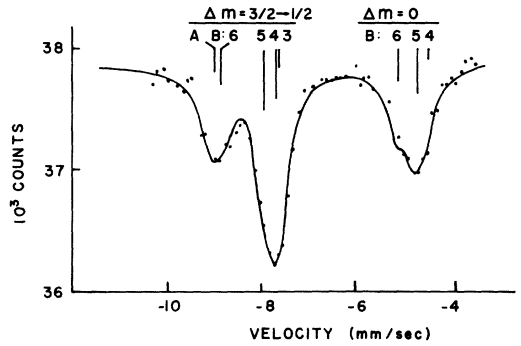

FIG. 5. Outer left-hand lines of the $Co_{0.2}Zn_{0.8}Fe_2O_4$ spectrum in an external magnetic field of 50 kOe. The curve drawn through the data points is the result of computer fitting. Vertical lines represent positions and relative intensities of the peaks used in the fitting procedure. Numerals above the lines indicate positions of peaks due to B-site Fe ions with 3, 4, 5, and 6 nearest-neighbor A-site Zn ions.

5. The dominant contribution to these $\Delta m = 0$ lines is found to correspond to the B-site Fe^{3+} spins, but the A-site Fe^{3+} spins are also found to be canted and produce relatively small but detectable $\Delta m = 0$ components. Near $x = 0$ the A-site canting angles are very small and their contribution to these lines is negligible. At $x = 0.4$ and 0.6 the spectra are described well by taking a canting angle $\theta_A \leq 20°$.

If the canting is uniform, that is, if all the spins on a given sublattice have the same canting angle, then the canting angle may be determined from the intensity ratio R for the $(\pm\frac{3}{2} \rightarrow \pm\frac{1}{2})$ and $(\pm\frac{1}{2} \rightarrow \pm\frac{1}{2})$ transitions given by

$$R = \tfrac{3}{4}(1+\cos^2\phi)/\sin^2\phi \qquad (3)$$

and from the measured resultant hyperfine field H_n using the expression

$$H_n = (H_0^2 + H_{eff}^2 - 2H_0H_{eff}\cos\theta)^{1/2} . \qquad (4)$$

In these expressions ϕ is the angle between the measured resultant hyperfine field and the direction of the external field H_0; H_{eff} is the hyperfine field with no external field; and θ is the canting angle of the Fe^{3+} spin with respect to the external field.

For a chemically disordered system such as $Co_{1-x}Zn_xFe_2O_4$ it is quite possible that the canting is not uniform but instead is locally dependent upon the statistical distribution of nonmagnetic neighboring ions. The data in this study, particularly for the $x = 0.6$ and 0.8 samples, give strong support to a localized canting picture at least as it applies to the B sublattice. With an external magnetic field, therefore, there is a distribution of spin projections in the field direction corresponding to the local distribution of nonmagnetic ions. The resulting spectrum is a superposition of spectra with hyperfine fields and intensity ratios for each spin projection given by Eqs. (3) and (4). The STH field is, in general, different for each local distribution of ions as discussed below in Sec. V. When canting is absent, the STH field components may be inferred from the observed line broadenings. This is not possible when canting is present and it may be difficult to include H_{eff} properly in Eq. (4). However, since STH contributions to H_{eff} are assumed to depend on a collinear alignment of spins, the STH field components may be negligible in the presence of large-angle canting.

Several theoretical models of localized canting have been proposed recently.[11–16] A model of particular interest to us has been developed by Rosencwaig[15,16] to calculate localized canting angles in substituted garnets. It is straightforward to apply his results for octahedrally coordinated sites in garnets to canting of octahedral B-site ions in substituted ferrites. For systems with a single magnetic constituent and for substitution only in the A sublattice, the canting angle θ_n for a B-site moment within the Rosencwaig model is given by

$$\cos\theta_n = \frac{(6-n) - 6\delta\cos\bar{\theta}}{[(6-n)^2 + (6\delta)^2 - 12(6-n)\delta\cos\bar{\theta}\,]^{1/2}} . \qquad (5)$$

In Eq. (5), n is the number of nearest-neighbor A sites occupied by zinc ions, $\delta = J_{BB}/J_{AB}$ is the ratio of the intrasublattice to intersublattice exchange constant, and $\bar{\theta}$ is the average canting angle for the B sublattice given by

$$\cos\bar{\theta} = \sum_{n=0}^{6} P(n,x)\cos\theta_n . \qquad (6)$$

$P(n, x)$ is the probability that a B-site Fe^{3+} ion has n nearest-neighbor Zn ions at A sites:

$$P(n,x) = \binom{6}{n}(1-x)^{6-n}x^n . \qquad (7)$$

It is interesting to note from Eq. (5) that when $n = 6$, $\cos\theta_6 = -\cos\bar{\theta}$. Thus B-site magnetic ions with all nearest-neighbor A sites occupied by zinc are oriented at an angle of $\pi - \bar{\theta}$ with respect to the magnetic field. Since, from Eq. (6), $\bar{\theta}$ varies between 0 and $\frac{1}{2}\pi$, the angle θ_6 will be $\geq 90°$. (Other θ_n may also be greater than 90° at higher concentrations.) For angles of $0 < \theta_n < 90°$ an external field subtracts from the B-site hyperfine field and for $\theta_n > 90°$ it adds.

Since larger local canting angles should occur for larger local concentrations of nonmagnetic ions we expect greater effects on the ME spectra at high zinc concentrations. This is indeed observed in the spectra in Figs. 1–5. The data show only slight line broadening in an external field for $x = 0$, 0.2, and 0.4. For $x = 0.6$ and 0.8, however, there is appreciable line broadening and for $x = 0.8$ there is evidence of large-angle B-site canting contribution

to the intensity of the A-sublattice spectrum. In fact, the probability of having 6 nonmagnetic near neighbors for the samples in this study is small except at $x = 0.8$, where $P(6, 0.8) = 0.26$. Therefore, we have treated the spectrum for $x = 0.8$ to check, at least qualitatively, the applicability of Rosencwaig's localized canting model. The procedure was to choose the angle $\bar{\theta}$ which best accounts for the additional intensity of the A-site spectrum from large-angle B-site canting and then self-consistently to solve Eqs. (5) and (6) to determine a value of δ. The best fit for $x = 0.8$ was obtained with $\bar{\theta} = 65°$ and $\delta = 0.15$. This analysis was also applied to the $x = 0.6$ spectrum using the value of δ obtained above to obtain a value of $\bar{\theta} = 52°$. The canting angles and configurational probabilities for these samples are shown in Table II.

The fit to the left-hand portion of the $x = 0.8$ spectrum at 50 kOe is shown in Fig. 5. The fitting procedure involved a summation of B-site spectral components for each value of θ_n with the spectral intensities and line positions properly calculated from Eqs. (3) and (4) along with a spectrum for the A sublattice. Adjustment was made for the small A-site canting discussed earlier.

It should be pointed out that Eq. (5), as discussed earlier, has been derived for systems with a single magnetic constituent and for substitution in only one sublattice and is, therefore, not strictly applicable to $Co_{1-x}Zn_xFe_2O_4$. The complication of having two magnetic species (Fe^{3+} and Co^{2+}) at B sites is diminished since J_{BB}(Co-Fe) and J_{BB}(Fe-Fe) are probably not too different in magnitude. Furthermore, our application of the model has been for large Zn concentrations where the J_{BB}(Fe-Fe) exchange is dominant because much of the Co^{2+} has been displaced.

Since we have made several approximations and our analysis using the Rosencwaig model is rather complex, the values obtained for δ and $\bar{\theta}$ may not be unique. However, the model of localized canting does appear to be confirmed. In particular, the line broadening and structural features of the spectra for the $x = 0.6$ and 0.8 samples in a magnetic field and the anomalously large intensity of the outer spectral lines of the 0.8 sample are quite adequately explained using this model.

TABLE II. Canting angles θ_n and fractions $P(n)$ for B-site Fe^{3+} ions with different numbers n of nearest-neighbor A-site Zn^{2+} ions calculated using Eqs. (5) and (6) with $\delta = 0.15$.

A	$Co_{0.4}Zn_{0.6}Fe_2O_4$	$(\bar{\theta} = 52°)$					
n	0	1	2	3	4	5	6
θ_n	~0°	~0°	~0°	14°	23°	68°	128°
$P(n)$	~0	0.04	0.14	0.28	0.31	0.19	0.05
B	$Co_{0.2}Zn_{0.8}Fe_2O_4$	$(\bar{\theta} = 65°)$					
n	0	1	2	3	4	5	6
θ_n	~0°	~0°	14°	18°	27°	53°	115°
$P(n)$	~0	~0	0.02	0.08	0.25	0.39	0.26

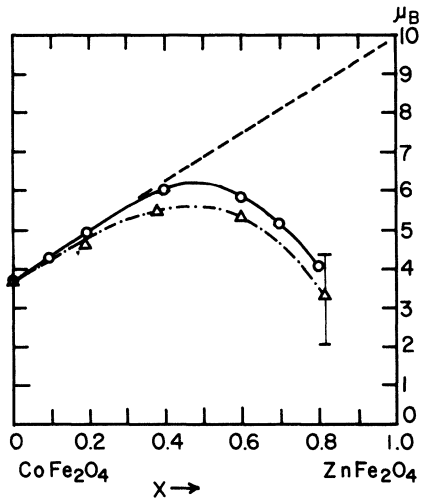

FIG. 6. Saturation moment per molecular unit in Bohr magnetons for $Co_{1-x}Zn_xFe_2O_4$ as a function of zinc concentration x. The measured curve (○) is by Guillaud (Ref. 6). The calculated curve (△) is obtained from the values given in Tables I and II used in Eq. (8). The straight-line extrapolation to 10 μ_B is the expected behavior for a Néel collinear arrangement of moments.

The appearance of $\Delta m = 0$ lines in the 4.2 °K spectrum of $CoFe_2O_4$ (Fig. 1) is somewhat surprising since such lines have not been observed in $NiFe_2O_4$.[26] However, it is not unreasonable to expect a small amount of canting due to the lack of a completely inverse structure in $CoFe_2O_4$. Also, the presence of the small A-site canting angles observed in these samples is assumed to arise because of the chemical disorder present at B-sites where two magnetic species are present.

Although no detailed fitting of the experimental data has been made for $x = 0.2$ and 0.4, we have calculated $\bar{\theta}_B$ for the B sites at these compositions from Eqs. (5) and (6) using a value of $\delta = 0.15$. The average canting angles calculated for $x = 0.2$ and 0.4 are $\bar{\theta} = 10°$ and 18°, respectively. Using the values of $\bar{\theta}_A$ obtained earlier we may now calculate the magnetization per molecular unit, M, from the cation distributions in Table I and the values of $\bar{\theta}_B$ given above:

$$M = (1+x+y)M_{Fe}\cos\bar{\theta}_B + (1-x-y)M_{Co}\cos\bar{\theta}_B - (1-x-y)M_{Fe}\cos\bar{\theta}_A - yM_{Co}\cos\bar{\theta}_A. \quad (8)$$

The magnetization calculated from Eq. (8) and assuming $M_{Fe} = 5\mu_B$ and $M_{Co} = 3\mu_B$ is plotted in Fig. 6. The agreement with Guillaud's data is reasonably close considering the assumptions made and

the experimental error involved. This agreement further confirms the conclusion that the primary cause of the deviation from the linear dashed curve in Fig. 6 is a result of the development of canting.

V. HYPERFINE FIELDS

A. Hyperfine Fields in Spinel Ferrites

The primary component of hyperfine fields at the nuclei of $3d^5$ ions arises from core polarization induced by the spin of the parent ion. When these ions are incorporated in the spinel lattice there are other field contributions which, although small compared with the core polarization field, are detected in ME and NMR measurements as both a shift in the average hyperfine field and as structure in the resonances. Covalent bonding of the metal ion with neighboring oxygen ions, STH fields induced by neighboring magnetic ions through oxygen bonds, deviations from a "spin-only" g factor, and dipolar fields all are expected to contribute to the distribution of fields. Of these, the dipolar field is estimated to have a small effect. Its main effect is expected to be a relatively small contribution to broadening of the lines. The effects of covalency and STH interactions are also expected to contribute to the detected isomer shifts.

The hyperfine field at octahedral B sites of inverse spinels is found to be roughly constant near 550 kOe, when the B-site iron ion has only Fe^{3+} neighbors at A sites. The A-site hyperfine fields are typically 10% less than this and the difference is usually attributed to covalency.[27] In spinels like Zn-substituted $NiFe_2O_4$, where some of the iron ions at A sites are replaced by nonmagnetic ions, several ME and NMR studies have revealed the presence of multiple hyperfine fields at Fe^{3+} nuclei in B sites.[2,20–22,28,29] A reduction of 14 kOe per A-site Fe neighbor replaced by Zn is found in $Ni_{1-x}Zn_xFe_2O_4$ at 77 °K.[23] The presence of multiple hyperfine fields at B sites has been attributed, in large part, to differences in STH contributions from the differing types of A-site near neighbors. In contrast, the distribution of fields at A sites has been found to be relatively small. This differing behavior for the A and B sites is not completely explained although Evans and Hafner[21] have suggested that the STH field at A sites from neighboring B sites is small. Streever[28] has compared the hyperfine fields at tetrahedral sites of $BaFe_{12}O_{19}$ and $CuFe_2O_4$ to obtain a value of only about 3 kOe per iron neighbor for the supertransferred field at the tetrahedral site.

The STH field components are expected to be strongly influenced by the superexchange coupling with neighboring ions and the magnetic moments of these ions. In the spinel structure, metal ions on octahedral B sites have strong superexchange interactions with six neighboring metal ions on tetrahedral A sites, while ions on the A sites are coupled strongly with 12 neighboring metal ions on the B sites. Through a given oxygen ion, a B-site ion interacts with only one A-site ion while an A-site ion interacts with 3 nearest-neighbor B-site ions. Because of their large separation distances (~ 3.5 Å), A-site ions are not expected to have a detectable interaction with other A-site ions. The B-site ions may interact with neighboring B-site ions only by direct overlap or through 90° superexchange paths. The distances and angles would lead to a weak interaction which seems to be confirmed by our earlier estimates of $J_{BB} \sim 0.15 J_{AB}$.

Huang *et al.*[30] have discussed STH field mechanisms which produce an *increase* in the hyperfine field of an Fe^{3+} ion coupled antiferromagnetically to another Fe^{3+} ion with a superexchange path of 180°. Thus it is expected that replacement of an A-site Fe^{3+} ion with a nonmagnetic Zn^{2+} ion will diminish the hyperfine field at a neighboring B-site Fe^{3+} ion. Presumably the 14-kOe reduction observed by Abe[23] is due to this effect. Also, it is expected that replacement of a B-site Co^{2+} ion in $CoFe_2O_4$ by an Fe^{3+} ion, which has a larger magnetic moment, will produce an increase of the STH contribution at an A site.

The analysis of multiple hyperfine field spectra must also take into account the localized canting reported in Sec. IV since the canting will produce an apparent distribution of fields when an external field is applied.

B. Distribution of Hyperfine Fields in $Co_{1-x}Zn_xFe_2O_4$

In $CoFe_2O_4$ [Figs. 1(a) and 1(b)] there is an obvious distribution of hyperfine fields at B sites both with and without an external field. As determined earlier, the canting angles for $x = 0$ are very small. Therefore, we may interpret the hyperfine field distribution in terms of STH field distributions. Since an analysis of multiple hyperfine fields in $CoFe_2O_4$ at 4.2 °K has not been made previously, it is of interest to carry out this analysis on our data. The outermost lines of the $CoFe_2O_4$ spectrum obtained at 4 °K in a field of 80 kOe in this study are shown in Fig. 7. Superimposed on the experimental spectrum are B-site spectral lines calculated by least-squares computer fitting using Eq. (7) to calculate the probabilities $P(n, y)$, where $y = 0.19$ is the fraction of Co^{2+} ions in "wrong" A sites as determined in Sec. III. For $y = 0.19$ the calculated intensity ratios are $P(0) : P(1) : P(2) : P(3) :: 0.41 : 0.58 : 0.34 : 0.11$. In the least-squares fit the adjustable parameters were the over-all intensity, base line, and peak locations. The peak widths were constrained to be the same but otherwise were varied by the fitting program to obtain a best fit. The hyperfine fields and isomer shifts obtained

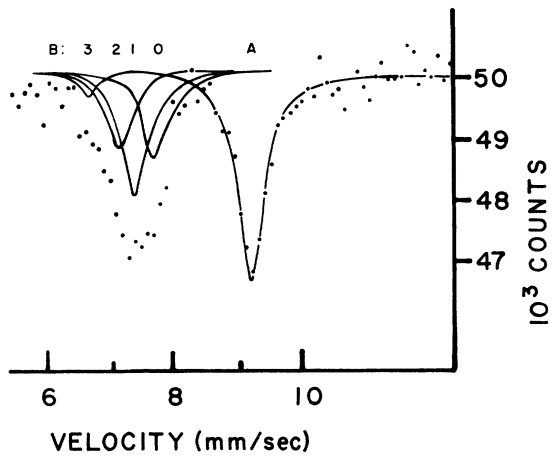

FIG. 7. Outer right-hand A- and B-site lines of the $CoFe_2O_4$ spectrum in an external magnetic field of 80 kOe. Results of computer fitting assuming the B-site line to be composed of a superposition of four lines are shown by solid curves. The numerals above the spectrum indicate positions of lines due to B-site Fe ions with 3, 2, 1, and 0 nearest-neighbor A-site Co ions, respectively.

from the calculated line centers are listed in Table III. For a B-site Fe^{3+} ion with six nearest-neighbor Fe^{3+} ions at A sites, the hyperfine field obtained is (548 ± 5) kOe. As for other spinel ferrites, the A-site field is about 10% less at (501 ± 5) kOe. By inspection of Table III we see that each Fe^{3+} A-site ion contributes, on the average, about 18 kOe more than a Co^{2+} ion to the hyperfine field at a nearest-neighbor B-site Fe^{3+} ion at 4 °K. This difference is comparable to that measured by Sawatzky *et al.*[2] near 100 °K but is almost twice the value obtained by their extrapolation to 0 °K. The magnitude of this difference is unexpected since both Fe^{3+} and Co^{2+} are magnetic and since only a 14-kOe difference was observed when nonmagnetic Zn^{2+} replaced an Fe^{3+} A-site ion in $Ni_{1-x}Zn_xFe_2O_4$. In fact, if additivity is assumed to hold, the data in Table III imply a field of only about 435 kOe for an $Fe^{3+}(B)$ ion surrounded by six $Co^{2+}(A)$ ions which, as we see shortly, is less than the B-site hyperfine field for $ZnFe_2O_4$ where an $Fe^{3+}(B)$ ion has six $Zn^{2+}(A)$ near neighbors. Similarly, as indicated in Figs. 1–4, the B-site linewidth decreases when zinc is added to the system in low concentrations. Again, this implies that replacement of an Fe^{3+} ion at an A site by Co^{2+} produces a larger reduction of the B-site hyperfine field than replacement by Zn^{2+}. The effects of canting at these low concentrations are assumed to be negligible.

As the zinc concentration is increased, the probability of obtaining larger local canting angles also increases. The observed line broadening or apparent distribution of hyperfine fields in an external magnetic field, then, results from a competition between the STH field distribution and the effects of the magnetic field. For larger concentrations of near-neighbor Zn^{2+} ions the $Fe^{3+}(B)$ hyperfine field is decreased because of STH effects. On the other hand, the canting angle is also larger and the nucleus experiences a smaller component of the external magnetic field. Since the external field subtracts from the B-site field, the B-site hyperfine field is reduced correspondingly less. The net result is a smaller distribution of hyperfine fields than would be present in the absence of an external field. Because of these competing effects and because at low concentrations (where canting might be neglected) there are apparently three kinds of ions, Zn^{2+}, Co^{2+}, and Fe^{3+}, present at A sites it is difficult to obtain the magnitude of the Zn^{2+} STH contribution at a B-site from a computer-fitting analysis such as that used earlier for $CoFe_2O_4$. We can, however, compare the hyperfine field obtained for $ZnFe_2O_4$ [(495 ± 5) kOe] with that obtained for a B-site ion in $CoFe_2O_4$ with six near-neighbor Fe^{3+} ions [(548 ± 5) kOe]. From this comparison we obtain a reduction of about 9 kOe for each Zn^{2+} ion which replaces an Fe^{3+} ion at an A-site neighbor. This value is slightly smaller than obtained by Abe in $Ni_{1-x}Zn_xFe_2O_4$ and is only one-half the 18-kOe change observed by us when Co^{2+} instead of Zn^{2+} is substituted at an A site.

C. Average Octahedral and Tetrahedral Fields

The variation of the average magnitude of H_{eff} at both A and B sites is shown in Fig. 8 and Table IV. These fields were determined from the separation between the centroids of the outermost peaks in each spectrum in an applied field with appropriate corrections for canting. For $x = 0.8$ and 1.0 the B-site fields were also determined from the zero-field spectra. The B-site field decreases almost linearly with increasing x while the A-site field first increases and then decreases again for $x > 0.5$. A similar variation of average hyperfine fields has been reported for $Ni_{1-x}Zn_xFe_2O_4$.[19] In that case,

TABLE III. Magnetic hyperfine fields in $CoFe_2O_4$ from computer fitting.

	A	$B(0)$	$B(1)$	$B(2)$	$B(3)$
H_{eff} (KOe)	501 ± 5	548 ± 5	530 ± 5	515 ± 5	491 ± 10
Isomer shift[a] (mm/sec)	−0.10 ± 0.05	0.0 ± 0.05	0.0 ± 0.05	0.0 ± 0.05	−0.14 ± 0.1

[a]Relative to ^{57}Fe in a Pt matrix.

however, the results are complicated by differences in sublattice magnetization at the temperature (77 °K) at which the data were taken. For large values of x, 77 °K is near or above the Néel temperature.

The decrease of the average B-site field with increasing zinc content is attributed to dilution of the STH field components from Fe^{3+} ions in neighboring B sites. Noting again that an A site has 12 nearest-neighbor B sites, and in $CoFe_2O_4$ roughly half of the B sites are Fe^{3+} and half are Co^{2+}, the initial increase of an A-site field corresponds to about 7 kOe per Fe^{3+} ion when Fe^{3+} replaces Co^{2+} at a B site. This is about twice Streever's[28] estimated contribution from an $Fe^{3+}(B)$ ion alone to the field at an A site. The subsequent reduction of $H_{eff}(A)$ above $x = 0.5$ is attributed to reduction in the STH field from B-site moments due to their increasing canting angles. Near $x = 1$, the B-site spins are paired antiparallel and the STH field components at A sites should cancel.

D. Isomer Shifts

For all samples the A-site isomer shifts are found to be about 0.1 mm/sec more negative than those for the B site. This shift is evident, for example, in the zero-field spectrum of $CoFe_2O_4$, Fig. 1(a). Similar differences between A- and B-site isomer shifts have been noted for other ferrites and have been given several interpretations including a partial $4s$-electron contribution to the $3d$-electron configuration and compression of the electronic wave function at A-site nuclei because of the smaller volume available for the ions at these sites. Within experimental error, the isomer shifts obtained from the present study do not vary as a function of zinc concentration. Similar behavior was noted for $Ni_{1-x}Zn_xFe_2O_4$.[19]

E. Discussion

If the distribution of hyperfine fields for $CoFe_2O_4$ ($x = 0$) is not considered, the general behavior of the hyperfine fields at A and B sites in $Co_{1-x}Zn_xFe_2O_4$ is similar to that for $Ni_{1-x}Zn_xFe_2O_4$. The average B-site field decreases almost linearly with increased zinc composition and a decrease of about 9 kOe is deduced for each Fe^{2+} ion replaced by Zn^{2+} at an A-site. This is to be compared with a roughly 14-kOe decrease in the nickel ferrite. In both the cobalt and nickel ferrite series the average A-site field first increases and then decreases as the zinc content is raised.

Some of the observed behavior of the hyperfine fields is unexpected. First of all, from the initial increase of $H_{eff}(A)$ in $Co_{1-x}Zn_xFe_2O_4$ we have deduced an increase of about 7 kOe for each Co^{2+} ion at a B-site which is replaced by an Fe^{3+} ion. This increase is twice that deduced by Streever for the contribution from an Fe^{3+} ion alone. Secondly, both our data and that of Sawatzky *et al.* on $CoFe_2O_4$ indicates that replacement of an Fe^{3+} ion at an A site by Co^{2+} *decreases* the field by an amount larger than when the Fe^{3+} ion is replaced by Zn^{2+}. Our analysis of 4.2 °K data gives a decrease of about 18 kOe for the $Fe^{3+} \rightarrow Co^{2+}$ replacement, whereas we find the $Fe^{3+} \rightarrow Zn^{2+}$ replacement results in a 9-kOe decrease. It is of interest to speculate about the cause of this unusual behavior of both A- and B-site fields. For example, the behavior could be explained in a simplified picture assuming that the STH field components at a B-site (A-site) Fe^{3+} ion from neighboring A-site (B-site) Co^{2+} or Fe^{3+} ions are in opposition and of roughly the same magnitude while zinc is assumed to make no contribution to the STH field. However, it is difficult to make a definitive differentiation of all the possible contributions to the STH fields. For one thing the reason for the relatively small STH field at an A-site ion from a neighboring B-site ion is still not understood. Also, it is expected that the contribution to the STH field from Co^{2+} at an A site will differ markedly from that at a B site because of large changes in the ionic crystalline field splittings.

Calculation of ionic dipolar effects is difficult because of the chemical disorder of Fe^{3+} and Co^{2+} ions at B sites, addition of a third component Zn^{2+}, and distortion from the ideal spinel lattice. We have used a computer program written by Schelling[31] and calculations by Johnson and Healy[32] to estimate these effects for an ideal spinel lattice. Dipole-field sums were taken over 20 successive spherical shells of 2-Å thickness about the central ion and only components in the direction of an external field were used. The result of these estimates is that dipole fields primarily broaden without shifting the spectral lines. The broadenings are much smaller than that expected from the STH field contributions. The largest estimated broadening as a function of zinc composition is about 5 kOe for the B-site peaks and about 2 kOe for the A-site peaks.

VI. TEMPERATURE DEPENDENCE

A number of the properties of zinc-substituted ferrites including the saturation magnetization have been explained by Gilleo[8] as being due to the presence of superparamagnetic clusters within the material. According to this model the ions order ferrimagnetically only within clusters which are separated magnetically from the matrix because all

TABLE IV. Magnetic hyperfine fields from centroid separations for $Co_{1-x}Zn_xFe_2O_4$.

X	0.0	0.2	0.4	0.6	0.8	1.0
$H_{eff}(A)$ (kOe)	501 ± 5	510 ± 5	515 ± 5	517 ± 6	508 ± 6	...
$H_{eff}(B)$ (kOe)	530 ± 5	522 ± 5	522 ± 5	511 ± 5	511 ± 5	495 ± 5

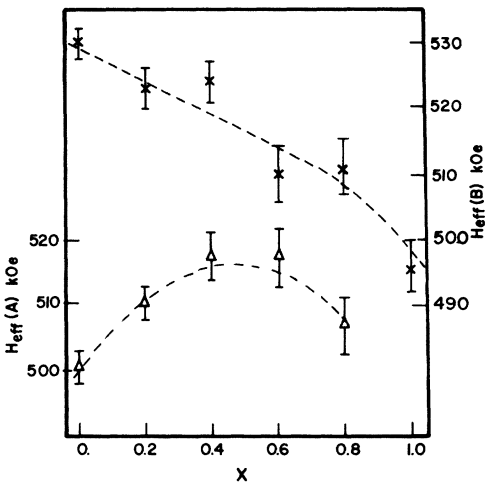

FIG. 8. Hyperfine magnetic field at A- (Δ) and B- ($\times$) site Fe ions in $Co_{1-x}Zn_xFe_2O_4$ as a function of zinc concentration. Field magnitudes are measured from separations between centroids of outer peaks in the spectra. The dashed lines are for the purpose of clarity and do not represent theoretical curves.

tetrahedral sites surrounding the cluster are occupied by nonmagnetic zinc ions. Each such cluster behaves like a superparamagnetic particle. Evidence for the presence of superparamagnetic clusters has been found in ME spectra as a central paramagnetic absorption peak superimposed on a magnetic hyperfine spectrum with broadened lines.[33-35] On the other hand, the spectral shapes obtained for several ferrites have been discussed in terms of relaxation effects which result when the atomic-spin relaxation frequency is comparable with the nuclear Larmor precession frequency.[19,36,37] For the Ni-Zn ferrite system, evidence has been presented that paramagnetic centers or superparamagnetic clusters do not explain the spectra in this system.[19]

At low temperatures (4 °K) the Co-Zn ferrite spectra taken in this study do not show the effects of relaxation or superparamagnetic clustering. The spectra at higher temperatures for the $x = 0.6$ sample are shown in Figs. 9 and 10. At a temperature of 198 °K the relative intensities of the innermost $\Delta m = \pm\frac{1}{2} \rightarrow \pm\frac{1}{2}$ lines are increased in intensity compared with the outer lines. At 295 °K the hyperfine pattern has coalesced into a broad peak with a quadrupole doublet superimposed on it. This quadrupole doublet remains above the Néel temperature as shown on the expanded plot in Fig. 10. The Néel temperature, taken as the point where only the paramagnetic quadrupole doublet remains, is found to be (322 ± 5) °K.

The general features of the spectra in the temperature range up to about 250 °K are similar to those for Ni-Zn ferrites,[19] $CaFe_2O_4$,[6] and others whose

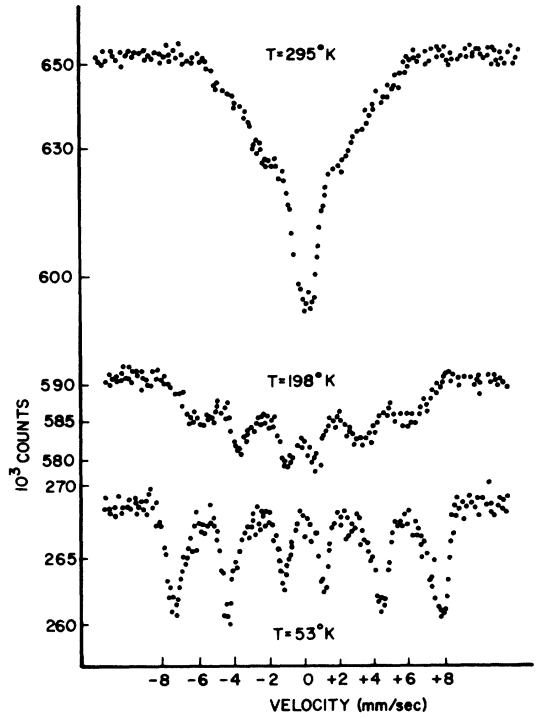

FIG. 9. Spectra of $Co_{0.4}Zn_{0.6}Fe_2O_4$ recorded at various temperatures below the Néel temperature. Spectra for $Co_{0.6}Zn_{0.4}Fe_2O_4$ show similar characteristics but at correspondingly higher temperatures.

characteristics have been attributed to relaxation behavior. Evidence for superparamagnetic clustering in this sample exists over only a small temperature range just below the Néel temperature where the ME spectra are similar to that shown for

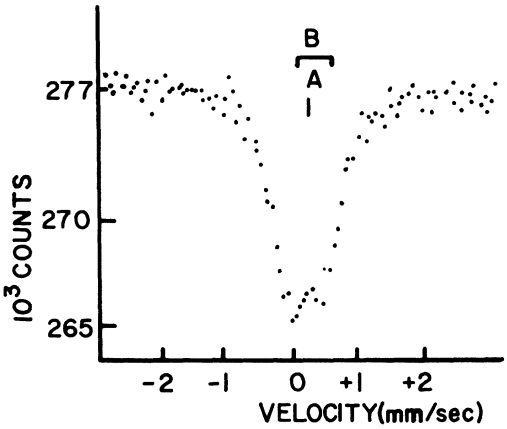

FIG. 10. Spectrum of $Co_{0.6}Zn_{0.4}Fe_2O_4$ taken with expanded velocity scale above the Néel temperature. Vertical lines indicate positions of peaks in the B-site quadrupole doublet and the unsplit A-site absorption line. The spectrum of $Co_{0.4}Zn_{0.6}Fe_2O_4$ above the Néel temperature shows similar characteristics.

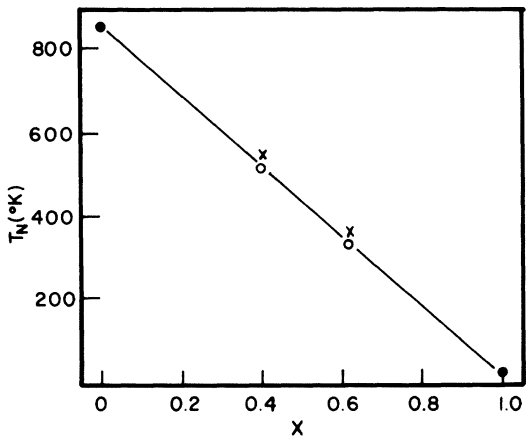

FIG. 11. Néel temperatures of $Co_{1-x}Zn_xFe_2O_4$ measured as a function of x. The points for $x=0$ and $x=1$ are from measurements of Sawatzky *et al.* (Ref. 2) and Varret *et al.* (Ref. 22), respectively. For intermediate zinc concentrations the points (×) are from the measurements of Booth and Crangle (Ref. 38) and the points (○) are from this study.

$T=295$ °K in Fig. 9. However, this behavior may result from some other mechanism such as a distribution of Néel temperatures.

The spectra for $x=0.4$ show similar behavior to that for $x=0.6$. The Néel temperature determined for this sample is (513 ± 5) °K. The Néel temperatures for these materials are plotted in Fig. 11. The points for $x=0$ and $x=1$ are from the measurements of Sawatzky *et al.*[2] and Varret *et al.*,[22] respectively. These points lie along a straight line and indicate an average increase of ~ 140 °K in T_N for each Zn ion replaced by a Co ion. The results of Booth and Crangle[38] are also shown in the figure. They obtain values of $T_N \simeq 540$ °K for $x=0.4$ and $T_N \simeq 360$ °K for $x=0.6$ from saturation-magnetization measurements in low fields.

As in the case of Ni-Zn ferrites, no evidence is found for quadrupole splittings in the data at low temperatures although such splittings are present just below and above the Néel temperature. Daniels and Rosencwaig[19] have given a possible explanation for this behavior in Ni-Zn ferrites in terms of chemical disorder in the samples which apparently masks the shifts in hyperfine field produced by the quadrupole interaction in the low-temperature spectra. The quadrupole doublets for the samples with $x=0.4$ and $x=0.6$ are both split by 0.43 ± 0.005 mm/sec. These doublets are attributed to B-site ions. The slight asymmetry in the doublet shown in Fig. 11 results from an unsplit absorption line attributed to A-site ions which have a more nearly cubic environment.

VII. CONCLUSIONS

Results of this study indicate that, except near $x=0$, where a small fraction of Co^{2+} ions appear to be at A sites, the structure of $Co_{1-x}Zn_xFe_2O_4$ is inverse. In the presence of an applied magnetic field applied parallel to the direction of γ-ray emission, $\Delta m=0$ lines are present in the ME spectra of all samples. The intensity of these lines increases with increasing x and for $x=0.6$ and 0.8 these lines are quite pronounced and the outer lines are broadened by the applied field. These results are explained on the basis of a localized distribution of canting angles among the spins of Fe^{3+} ions at octahedral (B) sites. Therefore, the decrease in magnetization of these materials as x is increased towards 1 is primarily associated with canting of the magnetic moments at B-sites.

A distribution of hyperfine fields is found for Fe^{3+} ions at B sites. This is attributed to differences in STH field contributions from neighboring A-site Fe, Co, and Zn ions. As has been observed for several spinel compounds, essentially no distribution in hyperfine fields is observed for Fe^{3+} ions at A sites. The distribution in STH field components for $CoFe_2O_4$ at 4 °K is unexpectedly large compared to the distribution found for the zinc-substituted samples. The hyperfine field at a B-site Fe^{3+} ion is reduced by about 18 kOe when a Co^{2+} ion is substituted for an Fe^{3+} ion at a neighboring A site, whereas substitution of a nonmagnetic Zn^{2+} ion reduces the field by only about 9 kOe. The increase of A-site hyperfine field for small x is attributed to increased STH fields as Fe^{3+} ions replace Co^{2+} ions at B sites, while the decrease at larger x is attributed to the effects of B-sublattice canting on this transferred field.

Data taken over a wide temperature range for $x=0.4$ and 0.6 reveal relaxation behavior. Near the Néel temperatures the line shapes are indicative of superparamagnetic clustering or a distribution of Néel temperatures. The effect of superparamagnetic clusters is not noted at lower temperatures. The Néel temperatures for the $x=0.4$ and $x=0.6$ samples are (513 ± 5) and (322 ± 5) °K, respectively, and lie on a linear extrapolation between the Néel temperature of $CoFe_2O_4$ and $ZnFe_2O_4$.

ACKNOWLEDGMENTS

The authors express their appreciation to Georgia Institute of Technology for the use of the Department of Physics superconducting magnet facility for some of the preliminary measurements in this study. The financial assistance of the Research Corp. (a foundation) is acknowledged for some phases of this study. The authors are also grateful to J. J. Krebs and V. J. Folen for many helpful discussions about the interpretation of results and about properties of cobalt-zinc ferrites, J. H.

Schelling for discussion on dipolar calculations, and G. H. Stauss for helpful comments on the text material. Finally we wish to thank H. W. Greer for assistance in taking the data.

[1]J. Smit and H. P. J. Wijn, *Ferrites* (Wiley, New York, 1959).
[2]G. A. Sawatzky, F. Van Der Woude, and A. H. Morrish, Phys. Rev. 187, 747 (1969).
[3]J. M. Hastings and L. M. Corliss, Phys. Rev. 104, 328 (1956).
[4]E. W. Gorter, Philips Res. Rept. 9, 1 (1954).
[5]G. Guillaud and H. Creveaux, Compt. Rend. 230, 1458 (1950).
[6]G. Guillaud, J. Phys. Radium 12, 239 (1951).
[7]Y. Ishikawa, J. Phys. Soc. Japan 17, 1877 (1962).
[8]M. A. Gilleo, J. Phys. Chem. Solids 13, 33 (1960).
[9]Y. Yafet and C. Kittel, Phys. Rev. 87, 290 (1952).
[10]D. H. Lyons, T. A. Kaplan, K. Dwight, and N. Menyuk, Phys. Rev. 126, 540 (1962).
[11]I. Nowik, Phys. Rev. 171, 550 (1968).
[12]I. Nowik, J. Appl. Phys. 40, 872 (1969).
[13]I. Nowik, J. Appl. Phys. 40, 5184 (1969).
[14]D. Lebenbaum and I. Nowick, Phys. Letters 31A, 373 (1970).
[15]A. Rosencwaig, Can. J. Phys. 48, 2857 (1970).
[16]A. Rosencwaig, Can. J. Phys. 48, 2868 (1970).
[17]G. A. Petitt and D. W. Forester, Bull. Am. Phys. Soc. 15, 207 (1970).
[18]N. S. Satya Murthy, M. G. Natera, S. I. Youssef, R. J. Begum, and C. M. Srivastava, Phys. Rev. 181, 969 (1969).
[19]J. M. Daniels and A. Rosencwaig, Can. J. Phys. 48, 381 (1970).
[20]J. J. Van Loef, Physica 32, 2102 (1966).
[21]B. J. Evans and S. S. Hafner, J. Phys. Chem. Solids 29, 1573 (1968).
[22]F. Varret, A. Gerard, and P. Imbert, Phys. Status Solidi 43, 723 (1971).
[23]H. Abe, M. Matsuura, H. Yasuoka, A. Hirai, T. Hashi, and T. Fukuyama, J. Phys. Soc. Japan 18, 1400 (1963).
[24]R. S. Hargrove and W. Kundig, Solid State Commun. 8, 303 (1970).
[25]Part of the measurements in external fields were made using the superconducting magnet facility at Georgia Institute of Technology and part using a Bitter-type solenoid at the Naval Research Laboratory high-magnetic-field facility.
[26]J. Chappert and R. B. Frankel, Phys. Rev. Letters 19, 570 (1967).
[27]J. C. M. Henning, Phys. Letters 24A, 40 (1967).
[28]R. L. Streever, Phys. Rev. 186, 285 (1969).
[29]S. L. Ruby, B. J. Evans, and S. S. Hafner, Solid State Commun. 6, 277 (1968).
[30]Nai Li Huang, R. Orbach, E. Šimánek, J. Owen, and D. R. Taylor, Phys. Rev. 156, 383 (1967).
[31]J. H. Schelling and G. T. Rado, Phys. Rev. 179, 541 (1969).
[32]R. J. Johnson and D. W. Healy, Jr., J. Chem. Phys. 26, 1031 (1957).
[33]P. Raj and S. K. Kulshreshtha, J. Phys. Chem. Solids 31, 9 (1970).
[34]W. Kundig, H. Bommel, G. Constabaris, and R. H. Lindquist, Phys. Rev. 142, 327 (1966).
[35]T. K. McNab, R. A. Fox, and A. J. F. Boyle, J. Appl. Phys. 39, 5703 (1968).
[36]H. Yamamoto, T. Okada, H. Watanabe, and M. Fukase, J. Phys. Soc. Japan 24, 275 (1968).
[37]S. W. Marshall and E. A. Samuel, Bull. Am. Phys. Soc. 14, 308 (1969).
[38]J. G. Booth and J. Crangle, Proc. Phys. Soc. (London) 79, 1271 (1962).

PHYSICAL REVIEW B VOLUME 4, NUMBER 11 1 DECEMBER 1971

Nuclear-Magnetic-Resonance Line-Shape Calculations for Polycrystalline Materials with bcc and fcc Symmetry*

S. Gade
Wisconsin State University, Oshkosh, Wisconsin 54901
(Received 16 June 1971)

The powder free-induction decays for body- and face-centered-cubic lattices of spins are calculated for spin values $I = \frac{1}{2}$ and 1. The powder decays are calculated by a computerized numerical integration of the formula of Lowe and Norberg as extended to include arbitrary spin. Only magnetic dipole-dipole interactions are considered. The powder decays are compared with $e^{(-a^2t^2/2)} \sin bt/bt$. The powder absorption curves are also calculated as the cosine transforms of the decay curves.

I. INTRODUCTION

Several formulas exist for the free-induction decay of a single crystal with an arbitrary number of spins fixed in spatial position, which were derived without a restrictive assumption about the form of the decay.[1-6] One of these single-crystal formulas, that of Gade and Lowe for arbitrary spin I, was used in a prior paper to calculate the free-induction decay curves for powders with simple cubic arrangements of the spins and $I = \frac{1}{2}$ and 1.[7] Since in the only case where experimental powder decays are available [CaF_2; simple-cubic lattice (SCL), $I = \frac{1}{2}$], good agreement exists between the theo-